



Spatial covariance of water isotope records in a global network of ice cores spanning twentieth-century climate change

David P. Schneider^{1,2} and David C. Noone^{1,3}

Received 12 March 2007; revised 29 May 2007; accepted 27 June 2007; published 20 September 2007.

[1] Estimating the spatial extent of past climate changes has been an ongoing challenge for paleoclimatology. For such estimates to be made with confidence, it is important to establish an understanding of the spatial coherence of proxy records during an interval of known climate change. We use water stable isotopes from high-resolution ice cores and twentieth-century observations of sea level pressures and sea surface temperatures to assess the covariance among isotopic records and its link to organized patterns of climate variability. Covarying signals in the cores are identified using empirical orthogonal function analysis. Results from regression analysis show that the leading signals are consistent with key climate patterns including the Northern Atlantic Oscillation and Southern Annular Mode and variability in tropical Pacific sea surface temperatures associated with the El Niño–Southern Oscillation. Patterns that have recently been identified in instrumental data, such as positive tropical Pacific SST anomalies associated with the negative phase of the SAM, are evident in the ice cores. These explanations for the variance of stable isotopes are consistent with recent studies using isotope-enabled general circulation models and provide a physical basis for interpreting the observed isotopic signals. While there is also a global change signal that is evident when analyzing the records collectively, there are some limitations in reconstructing global temperatures due to the geographic coverage of the available records and the current lack of modeling studies to explain the observed global-scale changes. Still, water stable isotope ratios preserved in ice cores provide a sufficiently rich sampling of large-scale climate variability that they can be more widely used in physically based paleoclimate reconstructions covering the last millennium and other periods.

Citation: Schneider, D. P., and D. C. Noone (2007), Spatial covariance of water isotope records in a global network of ice cores spanning twentieth-century climate change, *J. Geophys. Res.*, 112, D18105, doi:10.1029/2007JD008652.

1. Introduction

[2] Considerable effort has been devoted to developing millennial-length reconstructions of global and hemispheric temperatures based on information in natural archives such as tree rings, ice cores, and corals [e.g., Mann *et al.*, 1998; Esper *et al.*, 2002; Fisher, 2002; Jones and Mann, 2004; Moberg *et al.*, 2005]. Such reconstructions are important for estimating the range of climate variability that is incompletely sampled by instrumental records, and relevant to understanding the response of the climate system to anthropogenic and natural forcing. Several recent studies have focused on the limitations of climate reconstructions arising from statistical treatment of data and regression models [e.g., von Storch *et al.*, 2004; Esper *et al.*, 2005; Burger *et*

al., 2006; D'Arrigo *et al.*, 2006; Wahl *et al.*, 2006], and to a lesser extent, from incomplete understanding of and accounting for the physical relationship of proxy quantities to climate variability [e.g., Trenberth and Otto-Bliessner, 2003]. Here, we take a step toward reconciling the latter limitation, using the well-observed twentieth century as a test period for assessing the variance of water stable isotope ratios ($\delta^{18}\text{O}$ and δD) preserved in ice cores.

[3] Most multiproxy reconstructions with annual to decadal temporal resolution [e.g., Mann *et al.*, 1998; Esper *et al.*, 2002; Jones and Mann, 2004; Moberg *et al.*, 2005] have been based mainly on tree ring data; ice core $\delta^{18}\text{O}$ and δD records have been used, but generally constitute only a small fraction of the proxy databases. A chief cause of this imbalance is obviously the much larger number of tree ring records collected, especially from the Northern Hemisphere (NH) midlatitudes. The majority of reconstructions have focused on NH temperatures, with few data used to consider Southern Hemisphere (SH) or global mean temperatures. A secondary factor is a priori data selection criteria, which often include a strong positive correlation of the proxy quantity to local station or grid point temperature. The temporal correlation between ice core $\delta^{18}\text{O}$ and annual

¹Cooperative Institute for Research in Environmental Sciences, University of Colorado, Boulder, Colorado, USA.

²Now at National Center for Atmospheric Research, Boulder, Colorado, USA.

³Also at Department of Atmospheric and Oceanic Sciences, University of Colorado, Boulder, Colorado, USA.

mean temperature is often observed to be rather low. Explanations for this relationship commonly include the mismatch of temperature on precipitation days and the mean annual temperature, postdepositional alterations to the isotopic record (blowing snow and diffusion), and that much of the isotopic signature is imparted upstream of the deposition site, and may not necessarily be dominated by local conditions. That is, the isotopic ratio of precipitation represents a history of source conditions, rainout, and advection. While this ensures richness in the isotopic records, it can also confound the simple interpretation of records from a single site.

[4] Debate concerning the interpretation of δ ratios has been in part driven by investigations using atmospheric and coupled atmosphere-ocean general circulation model (GCM) simulations with isotopic tracers. Several of these studies have concluded that the local interannual δ -T relationship is weak [e.g., *Cole et al.*, 1999; *Noone and Simmonds*, 2002a; *Werner and Heimann*, 2002; *Hoffmann et al.*, 2005] because of air mass mixing, changes in source regions, and variations in transport pathways. However, some studies have suggested that organized patterns of atmospheric circulation variability are associated with significant regional anomalies in stable isotope ratios [*Noone and Simmonds*, 2002b; *Schmidt et al.*, 2007]. As such, it has been suggested that isotope-derived climate reconstructions be based on spatial patterns, rather than on local calibrations to temperature and precipitation. Some climate field reconstruction methods do account for spatial covariance [e.g., *Mann et al.*, 1998], however the physical linkage of the climate pattern to the proxy quantity is usually not transparent.

[5] Empirically, as in models, there is evidence linking isotopic variations to large-scale atmospheric circulation patterns. At low latitudes, monsoonal circulations strongly influence isotopic ratios over large regions [*Tian et al.*, 2003; *Vuille and Werner*, 2005; *Vuille et al.*, 2005]. At some low-latitude and midlatitude locations, isotopic records are correlated with tropical SST anomalies [*Bradley et al.*, 2003], and at Mt Logan in northwestern Canada, snow accumulation is correlated with the Aleutian Low and possibly teleconnected to tropical SST and ENSO variability [*Moore et al.*, 2002]. In Greenland, isotopic ratios are correlated with the North Atlantic Oscillation (NAO) [*White et al.*, 1997; *Vinther et al.*, 2003], and in the Antarctic, they are correlated with the analogous Southern Annular Mode (SAM) [*Schneider et al.*, 2005, 2006].

[6] The number of accurately dated, high-resolution ice core records is now sufficiently large to consider the covariance of δ ratios in the global domain, and the connections of δ variations to large-scale patterns of the atmospheric circulation. The establishment of such connections is particularly attractive from the standpoint of paleoclimate reconstruction, since low-frequency variability in the atmosphere can be efficiently described using just a few basis functions or modes. For instance, *Quadrelli and Wallace* [2004] developed a framework for describing more than 50% of wintertime extratropical Northern Hemisphere (NH) sea level pressure (SLP) variance in terms of a two-dimensional phase space defined by the Northern Annular Mode (NAM) and the Pacific–North America pattern (PNA), or alternatively, the North Atlantic Oscilla-

tion (NAO) and the North Pacific Index (NPI) pattern. *Trenberth et al.* [2005] analyzed mass distribution in the year-round, global domain, and identified the SAM as the leading pattern of variability, followed by the NAM/NAO and El Niño–Southern Oscillation (ENSO). The dominance of the SAM globally was also recognized by *Baldwin* [2001] in his analysis of global daily SLP observations.

[7] Patterns of temperature change project onto these modes, which vary on a range of timescales because of both intrinsic natural variability and external forcing [e.g., *Fyfe et al.*, 1999; *Hartmann et al.*, 2000; *Thompson and Solomon*, 2002; *Shindell and Schmidt*, 2004; *Sjoukje and van Oldenborgh*, 2006]. Much of the NH spatial-temporal pattern of temperature trends over the last 50 years projects onto the NAM or the essentially similar NAO [*Hurrell*, 1996; *Wallace et al.*, 1996; *Quadrelli and Wallace*, 2004]. Similarly, the 1969–1998 Antarctic trend pattern of cooling over the continent and warming on the Antarctic Peninsula is largely a SAM-related pattern [*Thompson and Solomon*, 2002]. However, the length of the instrumental record of patterns of variability is insufficiently long to adequately assess the significance of recent trends, yet such an analysis can be applied to proxy records.

[8] In this study, we seek to establish knowledge of the covariance among stable isotope records, identifying links to the major patterns of atmospheric circulation and their association with global-scale change. Thus our analysis is designed to assess the extent to which a few patterns of covariance among the ice cores relates to the atmospheric circulation framework discussed above. The isotopic patterns are identified in a consistent way as the atmospheric circulation patterns, using EOF analysis. Our analysis of ice core variability is limited to the overlap period of instrumental and ice core data, which places the greatest constraint on interpretations and corresponds to the period with the greatest number of records and least uncertainty in the ice core timescales. Understanding these linkages is an essential step toward confidently using these records in longer timescale reconstructions. Below, we first analyze the general characteristics of the stable isotope records by calculating the mean and principal components of 5-year average data. These time series are compared with the global mean temperature record and with significant regional climate changes. The second section of our study utilizes the annual resolution data to identify key interannual signals in stable isotopes, and uses historical sea level pressure data to link these signals to the major patterns of atmospheric circulation variability. We also highlight connections with the major patterns of SST variations, especially in the tropics, and finally highlight the differences between the low- and high- frequency covariance patterns in the records.

2. Data

2.1. Ice Cores

[9] Our ice core database contains stable isotope records from all of the major ice coring regions, including Greenland, Antarctica, and midlatitude and low-latitude glaciers, spanning a latitude range from 81°N to 87°S and an elevation range from 615 m to 7000 m above sea level (Figure 1 and Table 1). Most of the records are annually resolved, but several of the low-latitude records are only

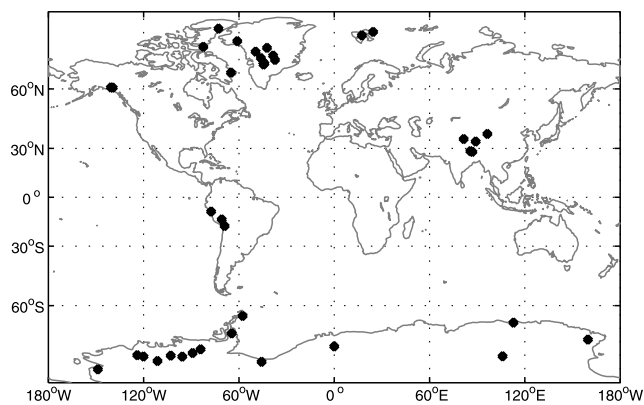


Figure 1. Locations of ice cores selected for this study indicated by black dots.

available as 5-year averages. Several of the records are obtained from public archives, and the rest have been kindly provided by individual investigators. Most of these records have been discussed individually in the literature, where detailed information on the core site, drilling procedures, dating methods, and original investigators' interpretations can be found (see Table 1 for references). Among the newest records in our database are Antarctic cores from the International Trans-Antarctic Scientific Expedition (ITASE) [Mayewski *et al.*, 2005] and Greenland cores from the Program on Arctic Regional Climate Assessment (PARCA) [Anklin *et al.*, 1998; Mosley-Thompson *et al.*, 2006]. Inevitably, the database cannot include all ice core records for several possible reasons: ongoing projects have not published results; data could not be obtained; some ice cores are too low resolution or too poorly age-constrained for this analysis; some records are “washed out” by summer melting; some records do not extend after 1980 or before 1900; some ice cores we are not aware of. The stacks (or averages) we use, such as the Fisher West Greenland, and the Law Dome 2000 composite, are those of the original investigators. We use the annual timescales as provided by the investigators.

[10] Selection of records involved some judgment; for instance, while the Vostok, Antarctica ice core [Petit *et al.*, 1999] is not well suited for this analysis because of its low sampling resolution and low snowfall deposition at the site, Vostok snowpit samples [Ekaykin *et al.*, 2002] achieve a much higher resolution allowing adequate dating to be obtained. Nonetheless, records from sites such as Vostok cannot be considered as reliably sampled and as precisely dated as those from sites in Greenland and West Antarctica where the snowfall is much greater. However, the tradeoff in fidelity at short timescales is worth the benefit gained by having one of the few detailed records from the vast Antarctic plateau.

[11] There have been reviews of subsets of these records [e.g., Fisher, 2002; Mosley-Thompson *et al.*, 2006; Mosley-Thompson and Thompson, 2003; Thompson *et al.*, 2006a; Yao *et al.*, 2006], however the present study is the first quantitative global-scale synthesis of stable isotope records from ice cores. Other hemispheric or global-scale compilations [e.g., Mann *et al.*, 1998; Fisher, 2002] have used the multiproxy approach, rather than the analysis of a single

proxy type, and we have included several additional isotopic records. As we seek to analyze the covariance among the records, we have not made an attempt to first screen them for correlation with local temperature or other climate parameters. Our analysis of ice core variability below is constrained to the overlap period of instrumental and ice core data, which is 1895–1990 for annual averages and 1860–1989 for 5-year averaged data. The data for 1860–1990 are complete except for several Arctic cores in the late 1980s, where we fill in the missing values with the mean of the previous 5 years. This has little effect on the covariance patterns discussed below, but may have an effect on representing the shift in the mean climate of the 1980–1990 decade. We standardize each record by subtracting its long-term mean (1860 to 1989 or 1895 to 1990) and dividing by the long-term standard deviation.

2.2. Climate Data

[12] We use the Hadley Centre-Climatic Research Unit version 3v of the global combined land-sea temperature record [Brohan *et al.*, 2006], which spans 1850–2006. Additionally, Hadley version 2, $5 \times 5^\circ$ gridded sea level pressure data are used in our analysis [Allan and Ansell, 2006]. These data have considerable uncertainty further back in time, especially in the data-sparse high latitudes [Allan and Ansell, 2006]. However, they are among the only gridded SLP data available prior to the beginning of the more comprehensive reanalysis data sets, and the major patterns of atmospheric circulation variability, NAM, SOI, PNA, SAM, are well represented [Allan and Ansell, 2006]. As these patterns are our main concern in this study, the Hadley SLP data are adequate for our purposes.

[13] We also use the Kaplan SST data set, which has a similar $5 \times 5^\circ$ resolution to the Hadley SLP2 data [Kaplan *et al.*, 1998]. However, the SST data are not globally complete; notably lacking are data from the middle to high-latitude SH. This data set consists of monthly anomalies from 1856 to present, and has increasing uncertainties back in time arising from observational data quality and data sparseness. The SLP and SST data were obtained from the Earth System Research Laboratory of the National Oceanic and Atmospheric Administration in Boulder, CO, and the temperature data were obtained from Climatic Research Unit of the University of East Anglia.

[14] To define the dominant patterns of variability we use the longest station-based indices available, ensuring the best data quality and consistency with previous research. As reported below, an alternative approach was taken to define some of the indices and patterns from empirical orthogonal function (EOF) analysis of the Hadley SLP data directly. However, results are somewhat clearer using the previously established indices. Therefore, instead of the NAM, we use the essentially similar winter NAO, defined by Hurrell's index back to 1866 [Hurrell, 1995]. Instead of the PNA pattern [Wallace and Gutzler, 1981] defined from reanalysis fields, we use the highly correlated winter season North Pacific Index (NPI), available back to 1901 from station data [Trenberth and Hurrell, 1994]. The Southern Oscillation Index (SOI) is the “SOI signal” defined by Trenberth [1984]. The NAO index, NPI, and SOI were all obtained from the Climate Analysis Section of the National Center for Atmospheric Research, Boulder, CO. For the SAM, we

Table 1. Information About the Ice Core Data Used in This Study, Including Data Sources and References of Original Publication, Listed in Order of Latitude From North to South^a

Site Name	Latitude, °N	Longitude, °E	Elevation, m	Type	5-Year	1-Year	Data Source	Key References
Agassiz 1977, pit	80.75	-72.83	1750	$\delta^{18}\text{O}$	y	y	NOAA Paleo WDC ^b	<i>Fisher and Koerner</i> [1994] and <i>Fisher et al.</i> [1995]
Austfonna	79.83	24.47	750	$\delta^{18}\text{O}$	y	y	E. Isaksson (personal communication, 2006) ^c	<i>Isaksson et al.</i> [2005]
Lomonsovfonna	78.85	17.42	1230	$\delta^{18}\text{O}$	y	y	E. Isaksson (personal communication, 2006)	<i>Isaksson et al.</i> [2005]
GITS PARCA	77.14	-61.09	1887	$\delta^{18}\text{O}$	y	y	E. Mosley-Thompson (personal communication, 2006)	<i>Mosley-Thompson et al.</i> [2006]
Devon 1999	75.42	-82.50	1800	$\delta^{18}\text{O}$	y	y	D. Fisher (personal communication, 2006)	<i>Patterson et al.</i> [1977] and <i>Zheng et al.</i> [2006]
N GRIP	75.10	-42.32	2919	$\delta^{18}\text{O}$	y	y	K. Andersen (personal communication, 2006)	<i>Andersen et al.</i> [2006]
NASA-U PARCA	73.84	-49.49	2369	$\delta^{18}\text{O}$	y	y	E. Mosley-Thompson (personal communication, 2006)	<i>Mosley-Thompson et al.</i> [2006]
White Summit	72.60	-38.50	~3200	$\delta^{18}\text{O}$ stack	y	y	NOAA Paleo WDC	<i>White et al.</i> [1997]
Fisher E Greenland	73.00	-34.00	~3000	normalized $\delta^{18}\text{O}$ stack	y	y	NOAA Paleo WDC	<i>Fisher et al.</i> [1995, 1996]
D2 PARCA	71.75	-46.16	2640	$\delta^{18}\text{O}$	y	y	E. Mosley-Thompson (personal communication, 2006)	<i>Mosley-Thompson et al.</i> [2006]
Fisher W Greenland	71.26	-37.70	~3000	normalized $\delta^{18}\text{O}$ stack	y	y	NOAA Paleo WDC	<i>Fisher et al.</i> [1995, 1996]
D3 PARCA	69.80	-44.00	2560	$\delta^{18}\text{O}$	y	y	E. Mosley-Thompson (personal communication, 2006)	<i>Mosley-Thompson et al.</i> [2006]
Raven PARCA	69.50	-44.50	2053	$\delta^{18}\text{O}$	y	y	E. Mosley-Thompson (personal communication, 2006)	<i>Mosley-Thompson et al.</i> [2006]
Penny 1995	66.50	-65.00	1900	$\delta^{18}\text{O}$	y	y	NOAA Paleo WDC	<i>Goto-Azuma et al.</i> [2002]
Logan NW Col	60.58	-140.58	5340	$\delta^{18}\text{O}$	y	y	NOAA Paleo WDC	<i>Holdsworth et al.</i> [1992]
Logan Eclipse 1996	60.51	-139.47	3017	$\delta^{18}\text{O}$	n	y	C. Wake (personal communication, 2006)	<i>Wake et al.</i> [2002]
Dunde	38.10	96.40	5325	$\delta^{18}\text{O}$	y	n	<i>Thompson et al.</i> [2006a]	<i>Thompson et al.</i> [1989]
Guilya	35.28	81.48	6200	$\delta^{18}\text{O}$	y	n	<i>Thompson et al.</i> [2006a]	<i>Thompson et al.</i> [1997]
Purogangri	33.92	89.08	6072	$\delta^{18}\text{O}$	y	n	<i>Thompson et al.</i> [2006a]	<i>Thompson et al.</i> [2006b]
Dasuopu	28.38	85.72	7000	$\delta^{18}\text{O}$	y	n	<i>Thompson et al.</i> [2006a]	<i>Thompson et al.</i> [2000]
Everest E Rongbuk	27.98	86.92	6500	$\delta^{18}\text{O}$	y	y	NOAA Paleo WDC	<i>Shugui et al.</i> [2002]
Huascarán 1, 2	-9.00	-77.50	6050	$\delta^{18}\text{O}$ stack	y	y	<i>Thompson et al.</i> [2006a], NOAA Paleo WDC	<i>Thompson et al.</i> [1995]
Quelccaya 1982, 2003	-13.93	-70.83	5670	$\delta^{18}\text{O}$ stack	y	y	<i>Thompson et al.</i> [2006a]	<i>Thompson et al.</i> [1985]
Sajama	-18.00	-69.00	6540	$\delta^{18}\text{O}$	y	n	<i>Thompson et al.</i> [2006a]	<i>Thompson et al.</i> [1998]
James Ross Island	-64.20	-57.67	1640	$\delta^{18}\text{O}$	y	y	A. Aristarain (personal communication, 2006)	<i>Aristarain et al.</i> [1990]
Law Dome 2000	-66.78	112.82	1370	$\delta^{18}\text{O}$ stack	y	y	T. van Ommen (personal communication, 2006)	<i>van Ommen and Morgan</i> [1997] and <i>van Ommen et al.</i> [2004]
Dyer Plateau	-70.66	-64.5	2002	$\delta^{18}\text{O}$	y	y	R. Mulvaney (personal communication, 2007)	<i>Thompson et al.</i> [1994]
Talos Dome	-72.80	159.75	2316	δD	y	y	NOAA Paleo WDC	<i>Stenni et al.</i> [2002]
Dronning Maud Land	-75.00	0.00	~2900	$\delta^{18}\text{O}$ stack	y	y	H. Oerter (personal communication, 2006)	<i>Graf et al.</i> [2002]
Siple Station	-75.92	-84.15	1054	$\delta^{18}\text{O}$	y	y	E. Mosley-Thompson (personal communication, 2006)	<i>Mosley-Thompson et al.</i> [1990]
01-5 ITASE	-77.06	-89.14	1239	$\delta^{18}\text{O}$	y	y	E. Steig and D. Schneider	<i>Schneider et al.</i> [2005]
00-5 ITASE	-77.68	-123.99	1828	δD	y	y	E. Steig and D. Schneider	<i>Schneider et al.</i> [2005]
01-2 ITASE	-77.84	-102.91	1336	$\delta^{18}\text{O}$	n	y	E. Steig and D. Schneider	<i>Steig et al.</i> [2005]
Vostok pits	-78.00	106.00	3488	δD	y	y	A. Ekaykin (personal communication, 2006)	<i>Ekaykin et al.</i> [2002]
01-3 ITASE	-78.12	-95.65	1620	δD	y	y	E. Steig and D. Schneider	<i>Steig et al.</i> [2005]
00-1 ITASE	-79.38	-111.23	1791	δD	y	y	E. Steig and D. Schneider	<i>Schneider et al.</i> [2005]
Berkner Island	-79.61	-45.72	886	$\delta^{18}\text{O}$	y	y	PANGAEA ^d	<i>Mulvaney et al.</i> [2002]
Siple Dome A core	-81.65	-148.81	615	δD	y	y	E. Steig (personal communication, 2006) and J. White (personal communication, 2006)	<i>Mayewski et al.</i> [2004]

Table 1. (continued)

Site Name	Latitude, °N	Longitude, °E	Elevation, m	Type	5-Year	1-Year	Data Source	Key References
Siple Dome B core	-81.65	-148.81	615	$\delta^{18}\text{O}$	y	y	E. Steig (personal communication, 2006) and J. White (personal communication, 2006)	Mayewski <i>et al.</i> [2004]
02-4 ITASE	-86.50	-107.99	2586	δD	y	y	E. Steig and D. Schneider	Jacobel <i>et al.</i> [2005]

^aAlso indicated is whether the data were used in the annual analysis and the 5-year average analyses (y, yes; n, no).

^bNOAA Paleo WDC: National Oceanic and Atmospheric Administration, World Data Center for Paleoclimatology, Boulder, Colorado.

^cPersonal communication refers to the data being directly obtained from an investigator.

^dPANGAEA: Publishing Network for Geoscience and Environmental Data, Bremen, Germany.

use an annual version of the station-based reconstruction of Jones and Widmann [2004] (annual version provided by J. Jones, personal communication, 2006). These indices capture the major patterns of global atmospheric mass distribution [Trenberth *et al.*, 2005] and have been widely discussed in the climate and paleoclimate literature. For the regression patterns discussed below, the indices have all been normalized to unit variance.

3. Results

3.1. General Characteristics

[15] The simple mean of the 5-year averaged normalized isotope records likely contains significant climate information. The mean also provides a guide to interpreting the EOF patterns discussed below. In Figure 2a, the means of the Arctic (15 cores, north of 60°N), low-latitude (8 cores, 40°N to 40°S), and Antarctic (15 cores, south of 60°S) records are displayed, along with the mean of all of the cores and the mean of the zonal means. The latter two time series are very similar ($r^2 = 0.92$), suggesting that our database is roughly balanced among the regions, although the polar regions get more weight relative to their area. Of the series, the Antarctic record is the most different from the others. The all-core mean is dominated by the Arctic and low-latitude signals. The Antarctic and Arctic records exhibit the most variability, consistent with the more variable and sensitive climate of the polar regions compared with the low latitudes. The low-latitude record, characterized by a steady increase, is similar to the “tropical” composite of Thompson *et al.* [2006a]. All series have a positive trend for the 1860–1989 period. The greatest increase in the all-core mean occurs in the 1920–1940 period. This is consistent with rapid climate warming in the Arctic at that time [e.g., Box, 2002]. The latter twentieth-century warming period is not well covered by our database, which ends in 1989. However, the low-latitude data to 2000 show a continued increase [Thompson *et al.*, 2006a], while the Antarctic data on average show a post-1990 decrease, attributable to the positive trend in the SAM [Schneider *et al.*, 2006]. There are insufficient data from the Arctic to characterize the last decade of the twentieth century, though the 1960–1989 period shows a decline, probably associated with the positive trend in the NAO and cooling in western Greenland and the Baffin Bay [Chapman and Walsh, 1993; Box, 2002].

3.2. Principal Component Regression

[16] While the simple mean of the records provides general information, a principal component or EOF analysis

can identify patterns of significant covariance among the records, and is a convenient way to characterize the variability in our geographically distributed database. Indeed it is of primary interest to assess whether covariance among the isotope records reflects large-scale climate variability; an appealing postulation that need not hold true. The ice core records are distributed unevenly in space, and therefore only regionally significant patterns may be resolvable. On

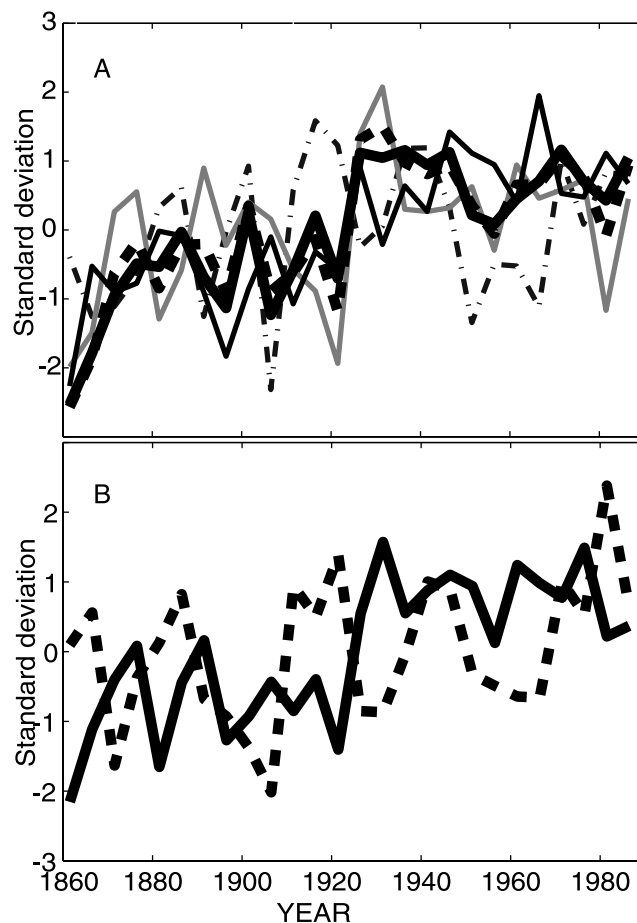


Figure 2. (a) Five-year averages of the standardized ice core isotopic time series for Arctic cores (gray solid line), low-latitude cores (black, thin solid line), Antarctic cores (black dash-dotted line), mean of all the cores (black, heavy solid line), and mean of the zonal means (black, heavy dashed line). (b) Standardized first (solid line) and second (dashed line) principal components of 5-year averaged ice core isotopic time series.

Table 2. Correlations of Leading PCs and 5-Year Averaged Ice Core Data Over 1860–1989 and Correlations of Leading PCs and Annual Average Ice Core Data Over 1895–1990^a

Site Name	PC1 5-Year	PC2 5-Year	PC1 Annual	PC2 Annual	PC3 Annual	PC4 Annual	PC1 High-Pass	PC2 High-Pass	PC3 High-Pass	PC4 High-Pass
Agassiz 1977, pit	0.31	−0.42	0.06	−0.14	0.08	−0.19	−0.03	−0.17	0.11	0.19
Austfonna	0.57	0.24	0.20	0.12	0.43	0.03	0.08	−0.31	−0.29	−0.33
Lomonsovonna	0.43	0.18	−0.11	0.10	−0.03	0.18	−0.09	0.03	−0.46	−0.13
GITS PARCA	0.21	−0.43	0.02	−0.11	−0.32	−0.36	−0.13	0.06	−0.01	0.04
Devon 1999	0.56	−0.50	0.24	−0.33	0.02	−0.26	0.07	0.01	0.02	0.09
North Grip	0.25	−0.82	0.50	−0.32	−0.41	−0.06	0.60	−0.11	0.03	0.09
NASA-U PARCA	−0.12	−0.66	0.50	−0.30	−0.50	0.16	0.70	−0.13	−0.25	−0.06
White Summit	0.72	−0.23	0.89	0.09	−0.03	0.06	0.87	−0.04	0.19	−0.04
Fisher E Greenland	0.44	0.08	0.67	0.33	0.02	−0.04	0.69	0.13	0.27	−0.09
D2 PARCA	0.62	−0.47	0.78	−0.09	−0.10	−0.04	0.71	−0.17	−0.22	−0.21
Fisher W Greenland	0.72	−0.20	0.79	0.02	0.18	−0.04	0.78	−0.13	0.21	−0.20
D3 PARCA	0.80	−0.12	0.71	−0.10	0.24	−0.03	0.73	−0.33	0.11	−0.08
Raven PARCA	0.34	0.17	0.00	0.02	0.17	0.14	−0.09	−0.11	−0.25	0.06
Penny	0.08	−0.65	0.09	−0.40	−0.30	0.12	0.09	−0.17	−0.33	−0.47
Logan	0.14	0.18	0.07	−0.02	−0.17	−0.07	0.19	0.14	−0.21	0.57
Eclipse 1996			0.03	0.09	0.19	0.44	−0.15	0.06	0.11	−0.26
Dunde	0.56	0.03								
Guilya	0.50	0.34								
Purogangri	0.19	0.29								
Dasuopu	0.56	0.14								
Everest E Rongbuk	0.44	0.24	−0.08	0.13	0.31	−0.42	−0.23	0.08	0.43	−0.39
Huascaran 1, 2	0.17	−0.02	0.12	0.16	−0.11	−0.05	0.03	0.27	0.11	−0.02
Quelccaya 1982, 2003	0.27	0.05	−0.06	0.03	0.05	−0.44	−0.33	−0.10	0.16	−0.42
Sajama	0.19	−0.24								
James Ross Island	−0.55	0.02	−0.17	0.19	−0.00	−0.76	−0.08	0.17	0.57	0.04
Law Dome 2000	0.10	0.21	−0.06	−0.10	0.13	−0.11	−0.10	−0.15	0.03	−0.19
Dyer Plateau	0.41	0.54	0.11	0.42	0.38	0.08	0.14	0.12	0.41	0.15
Talos Dome	−0.17	−0.14	−0.07	0.10	−0.21	−0.35	0.07	−0.03	0.23	−0.04
Dronning Maud Land	0.53	−0.01	0.37	0.07	0.48	−0.20	0.07	−0.08	−0.13	−0.55
Siple Station	0.08	0.35	0.16	0.59	−0.41	0.11	0.34	0.58	−0.14	0.06
01-5 ITASE	0.38	0.66	0.11	0.67	−0.08	0.05	0.13	0.66	−0.14	−0.17
00-5 ITASE	−0.16	0.07	−0.02	0.28	−0.21	−0.38	−0.18	0.35	−0.07	−0.62
01-2 ITASE			−0.17	−0.05	0.20	−0.15	−0.20	−0.49	−0.08	0.03
Vostok pits	0.09	0.54	0.13	0.30	0.45	0.14	0.08	−0.31	0.21	0.03
01-3 ITASE	0.04	0.47	0.13	0.55	−0.25	0.01	0.24	0.54	−0.20	0.08
00-1 ITASE	0.09	0.48	0.16	0.67	−0.21	−0.02	0.24	0.64	0.15	−0.10
Berkner Island	0.08	0.37	−0.31	0.43	−0.23	0.11	−0.16	0.53	−0.31	−0.09
Siple Dome A core	−0.17	−0.17	0.06	−0.06	−0.27	−0.19	0.11	0.30	−0.01	−0.01
Siple Dome B core	−0.10	−0.31	0.08	−0.35	0.08	−0.16	0.05	−0.31	−0.46	0.08
02-4 ITASE	−0.30	0.15	−0.10	0.12	−0.30	0.39	0.18	0.16	−0.56	0.14

^aValues in bold type are significant at the 95% level or better by a two-tailed t-test accounting for autocorrelation.

the other hand, isotopic records result from more spatially disperse mechanisms compared to, say, tree rings, and thus integrate more than the local environmental variability.

[17] We apply empirical orthogonal function (EOF) analysis to the 5-year averaged standardized ice core time series, which is equivalent to EOF of the correlation matrix [e.g., von Storch and Zwiers, 2001]. Leading principal components (PCs) are calculated by projecting the EOFs onto the standardized data. In our terminology, EOF refers to the spatial pattern, while the PCs refer to the time series describing the amplitudes of the patterns. To represent the EOFs in recognizable terms, we list the correlation of each core with the corresponding PCs in Table 2.

[18] EOF1 represents the most efficient way to describe the largest possible amount of variance in the database. EOF1 of the isotopic database explains 15% of the total variance, and it is associated with variance common to cores from across all of the latitudes. All cores have positive weights except for James Ross Island (Table 2). One similarity among the cores is that they all, except for James Ross Island, have generally positive twentieth-

century trends, and this is reflected the corresponding PC1 (Figure 2b). PC1 is significantly correlated with the simple mean of the cores ($r = 0.87$), and likewise is dominated by the Arctic and low-latitude cores.

[19] EOF2 explains 13% of the variance, and it is characterized by negative weights with several northwest Greenland and Canadian Arctic cores, and positive weights with the majority of Antarctic and Tibetan cores. The Antarctic signal is dominant; PC2 is correlated with the mean of the Antarctic cores at $r = 0.63$. PC2 shows a positive trend (Figure 2b).

[20] The leading two EOFs place the Arctic cores into two groups—those showing a decline from around 1930 to 1989, and those showing an increase. For illustration, the Greenland cores with the strongest weights in EOFs 1 and 2 are plotted in Figure 3. The several cores with a negative EOF2 weight are from northwest Greenland sites and from across the Baffin Bay in the Canadian Arctic ice caps. Arctic cores with strong weights in EOF1 are those from the Summit site and D2 and D3 sites in central Greenland. The first group of sites encompasses a region where climate

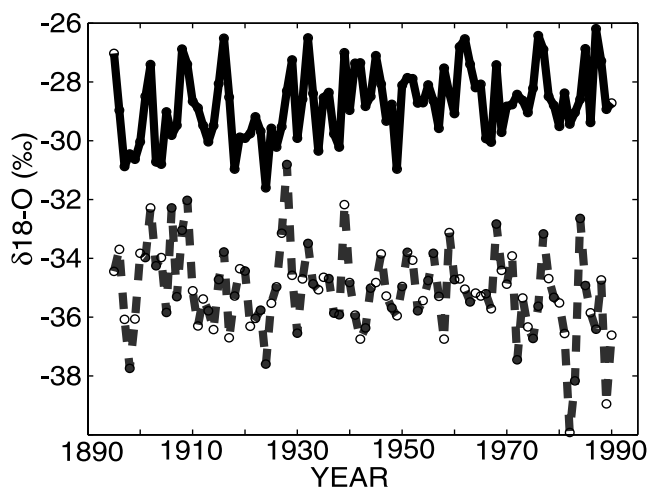


Figure 3. Two isotopic records from Greenland. Circles indicate the annual values. The solid line is core D3, which is associated with PC1 of the 5-year averaged ice core data. The dashed line is core NGRIP, which is associated with PC2 of 5-year averaged data. Both are associated with PC1 of annual and high-pass filtered data.

variability is dominated by the NAO [e.g., Hurrell, 1995], and where temperatures from 1960–1990 decreased [Box, 2002]. Although the entire region is affected by the NAO, including the Summit sites grouped into EOF1 [White *et al.*, 1997], there are clearly differing degrees of sensitivity among the isotope records. Efforts to average all Greenland cores together for the purposes of climate reconstruction, such as our exercise above and that of Andersen *et al.* [2006], may cause loss of information and should therefore proceed with caution.

[21] The EOF analysis has identified both common signals among the cores and dominant regional signals that are obscured in the means. To assess whether isotope records are a good basis for reconstructing global-scale temperature, we use a least squares principal component regression (PCR) to model the global change record, as captured in the surface temperature, as a function of the leading ice core principal components. Only the coefficients for the first two PCs, those discussed above, are significant at 95% by the t-test. These PCs account for 28% of the total variance in the ice core database and much more at many individual sites. Both PCs show a twentieth-century increase, however the timing is somewhat different. PC1 is characterized by a step-change like signal, showing a rapid increase from the 1920s to the 1930s. PC2 shows more variability on top of a steadier increase, with the most rapid increase earlier than PC1, around 1910, and another rapid increase from around 1965 to 1980. The modeled time series using just these two predictors explains 62% of the variance in the global mean temperature record (Figure 4).

3.3. Summary of Low-Frequency Variability

[22] The available isotope records from the entire range of latitudes predominantly show a twentieth-century increase, consistent with large-scale climate warming. Isotope ratios are also consistent with climate change in the Baffin Bay region, one of the most anomalous regions with respect to

global warming [Chylek *et al.*, 2004]. Notably, however, several cores near the eastern Pacific, such as Mt Logan, Quellccaya, and Huscaran, make little contribution to the first two EOF/PC pairs and hence to explaining the global signal. Furthermore, a shortcoming in explaining the global temperature record with the current set of ice core data is the relatively large residual in the last 5-year time period, 1985–1989. This result may be due to the truncation of several of the Arctic records in the early 1980s, which we extended by using the mean of the previous 5 years, which results in likely unrealistic constant proxy values at a time when the global mean temperature changed rapidly. Also, the geographic distribution of the ice cores does not overlap significantly with the regions that warmed most in the 1980s.

[23] To partially test the first possibility, we excluded those cores with early end dates and repeated the analysis, using data through 1994. This analysis included 28 records, rather than the original of 38 records. Although a similar good fit to the global temperature record through about 1980 was found, the period post-1980 still exhibited a large residual. It is likely then that the geographic distribution contributes to the disagreement.

[24] As discussed further below, the distribution is such that the cores are dominated by the NAO and SAM signals. Therefore the records may reflect the component of global change that is congruent with these patterns of variability, while not the remainder of any climate change signal. As noted above, a significant part, but not all, of the NH temperature change signal can be represented as a projection onto the major patterns of variability. For instance, despite the increase in the NAO from the 1970s through the 1990s, the NAO index has been more neutral in recent years, and recent discussions have deemphasized its role in explaining ongoing warming across the Arctic [e.g., Turner *et al.*, 2007].

3.4. Interannual Variability

[25] We apply EOF analysis to the database of 35 annual resolution ice core records, covering 1895–1990. The lead-

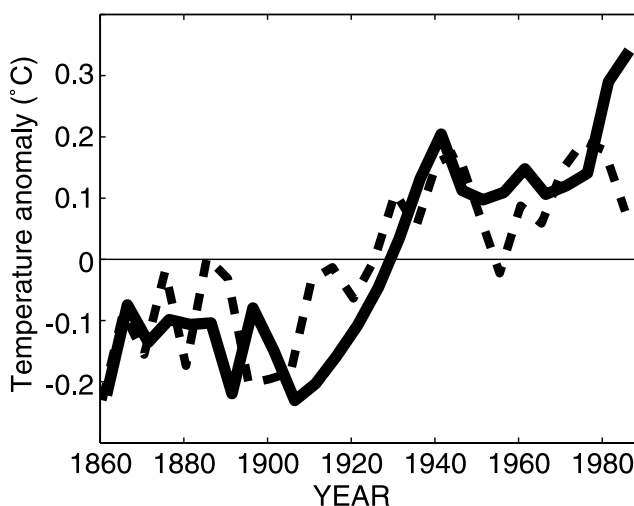


Figure 4. Global mean temperature record (solid line) and an estimation of it using multiple linear regression of the two leading ice core PCs at 5-year resolution (dashed line).

ing four modes explain 12%, 9%, 6.7%, and 6.4% of the variance, respectively. The correlations of the leading PCs with the individual ice cores are shown in Table 2. Figure 5 shows the regression maps of SLP and SST fields regressed upon each ice core PC, along with similar regressions with some major climate indices. The first EOF primarily captures a Greenland signal, with the strongest contributions from the White and Fisher stacks of central Greenland. The second EOF corresponds to several cores from West Antarctica. The third and the fourth EOFs are more regionally mixed, not clearly dominated by one region. The fourth mode is most highly correlated with a number of cores from Antarctica and Quelccaya. The remaining EOFs tend to be dominated by a single to a few cores, and thus do not show significant patterns of covariance. The level of variance explained by our leading modes is similar to that found by Fisher [2002] for a 40–50 member temperature proxy database containing ice core and tree ring time series. It is above the amount that would be explained in a database containing only white and red noise. Here we consider whether the first four isotope EOFs are consistent with known organized patterns of atmospheric circulation variability and variations in SST.

[26] The regression pattern (Figure 5) of isotope PC1 in Hadley SLP shows a classic NAO pattern. Although the anomalies in the PC1 pattern are somewhat weaker, the North Atlantic seesaw is clearly evident, showing the oscillation between the Azores and the Iceland to Svalbard region. The two patterns have a high area-weighted spatial correlation (Table 3). This result is consistent with the location of the cores in Greenland.

[27] In SST, the regression pattern associated with isotope PC1 is also NAO-like, but the correlation is not as strong as the SLP pattern correlation. The region of positive SST anomalies to the south of Greenland and near Iceland is clearly evident in the regression pattern (showing the negative polarity of the NAO), along with negative SST anomalies near northern Europe and northeastern North America.

[28] For comparison to the NAO, we also calculated the NAM pattern from the Hadley SLP2 data directly, as the first EOF of annual SLP anomalies from 20°N to 90°N. This pattern is more hemispheric in character than the NAO, with less weighting in the North Atlantic. The ice core regression pattern is more highly correlated with the NAO pattern than the NAM ($r = 0.82$ versus 0.66), probably reflecting the predominance of core locations in Greenland.

[29] The regression pattern of isotope PC2 in Hadley SLP does not resemble a classic pattern in the sense of the NAO, ENSO, or SAM. However, the pattern resembles the wave-3 pattern in the Southern Ocean, which has been recognized as one of the main modes of interannual variability in the high-latitude Southern Hemisphere [e.g., Mo, 2000]. Schneider *et al.* [2004] found that the wave-3 pattern is second to the SAM in the amount of surface temperature variance explained in West Antarctica. The region of largest SLP anomalies, from 120°W to 60°W, is consistent with the wave-3 pattern's deepest center of action and also with the location of the ice cores in West Antarctica that primarily contribute to the PC2 signal. The regression pattern of isotope PC2 in SST is not particularly distinctive, though it is most closely correlated with that of the NPI.

[30] The regression pattern of isotope PC3 in Hadley SLP is best correlated with the SAM pattern, and moderately with the NAO and NPI patterns. As the third and fourth eigenvalues overlap when taking into account the spatial-temporal autocorrelation of the data [North *et al.*, 1982; Bretherton *et al.*, 1992], it is likely that the real climate signals are mixed among the patterns that emerge from the isotope analysis. Thus it is not surprising that we do not find a pure, easily recognizable pattern associated with each of the isotope EOFs. We performed Varimax-rotated EOF analysis in an attempt to find “purer” modes with relaxed orthogonality constraints, but this resulted in highly localized weightings on just one or two ice cores due to the high local variance (perhaps “noise”) in each individual core, rather than the spatially coherent patterns we are interested in. Thus, in our case, regular EOF analysis was the better choice. Also, it should be noted that the well known organized patterns of variability themselves, the NAO, NPI, SAM and ENSO, are not strictly linearly independent. For instance, the PNA/NPI pattern is often considered a high-latitude manifestation of ENSO [e.g., Zhang *et al.*, 1996], and the wave number-3 and Pacific–South American patterns in the Southern Hemisphere are often similarly related to ENSO [e.g., Ribera and Mann, 2003; Venegas, 2003].

[31] The SST regression pattern of isotope PC3 is remarkably well correlated with that of the SOI, displaying strong weights in the tropical and North Pacific. Despite the ambiguity in interpreting the isotope PCs as representing pure climate signals, the results for the SLP and SST patterns are consistent with one another, underscoring the importance of the spatial organization of the atmospheric circulation and SST anomalies in determining isotopic variance.

[32] The regression pattern of isotope PC4 in Hadley SLP closely resembles the SAM pattern. The zonal seesaw in the high-latitude SH is clearly evident, with large anomalies over the Antarctic balanced by weaker anomalies of the opposite sign over broad areas of the southern ocean. The location of PC4-weighted cores in Antarctica is consistent with the pattern. An interesting result is the weighting of the Quelccaya core in the fourth isotope EOF. This has been primarily interpreted as an ENSO-sensitive site with an Atlantic moisture source [Vuille *et al.*, 2003; Vuille and Werner, 2005]. As with the NAM/NAO, we also calculated the SAM as the first EOF of SLP from 20°S to 90°S. Although the correlation with the isotope PC4 regression pattern is good ($r = 0.76$), the correlation with the station-based pattern is better (Table 3). This may relate to data quality in the sparsely observed high-latitude SH, which Jones avoided by constructing the pre-1950s index with only non-Antarctic, midlatitude station data.

[33] The SST pattern associated with the SAM may help to provide an explanation for the Antarctic–South American connection. The negative phase of the SAM is associated with positive, El Niño–like SST anomalies in the tropical Pacific. Such a relationship has recently been discussed in the literature [L'Heureux and Thompson, 2006] based on modern reanalysis data. L'Heureux and Thompson [2006] show that 25% of the interannual variance in the DJF SAM index is explained by linear correlation with the cold tongue index. Vuille and Werner [2005]

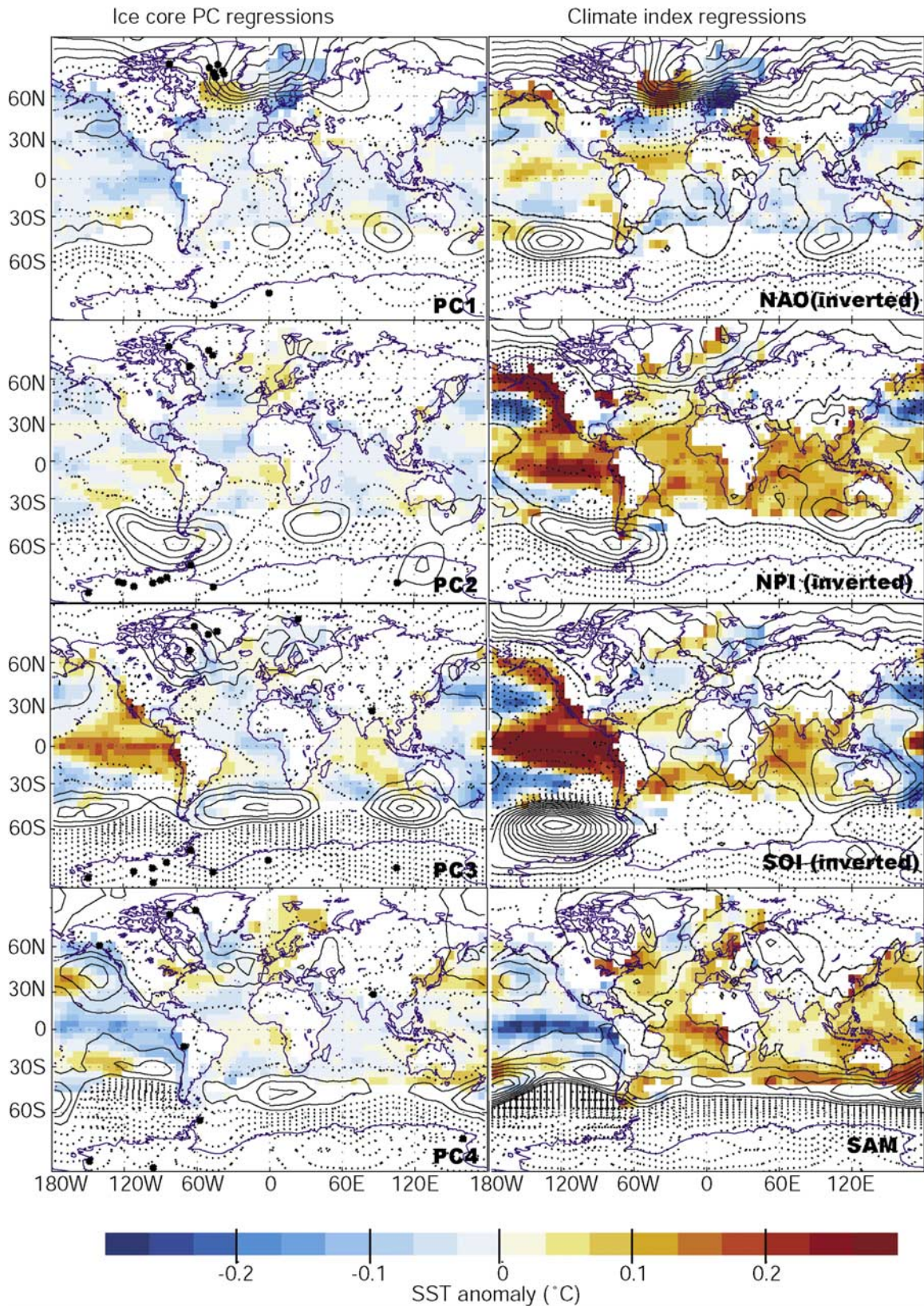


Figure 5. Regression maps of the indicated (left) standardized annual ice core PCs and (right) standardized climate indices versus Hadley SLP2 anomalies (contours, interval 0.1 hPA/std dev, positive values solid and negative values dashed) and Kaplan SST anomalies (colors, K) over 1895–1990. The sites with significant correlation with the respective PC are indicated by black dots.

Table 3. Spatial Correlations of the Regression Patterns in SLP and SST Shown in Figures 5 and 6

	Interannual				High-Pass Filtered			
	NAO	NPI	SAM	SOI	NAO	NPI	SAM	SOI
	<i>SLP</i>							
PC1	-0.83	0.46	0.42	-0.03	-0.72	0.02	0.28	0.25
PC2	0.10	0.48	-0.05	-0.17	0.37	0.25	-0.19	-0.20
PC3	-0.48	0.42	0.70	-0.01	-0.17	0.46	-0.40	-0.74
PC4	0.15	0.09	0.81	0.58	0.42	-0.50	0.61	0.52
	<i>SST</i>							
PC1	-0.36	0.50	0.19	0.40	-0.34	0.21	0.41	0.32
PC2	0.04	-0.36	0.24	-0.32	0.13	-0.38	-0.31	-0.38
PC3	-0.08	0.69	-0.66	-0.92	-0.26	0.73	-0.83	-0.88
PC4	0.39	-0.72	0.54	0.75	0.72	-0.78	0.74	0.78

use a similar measure of tropical SST, the Nino 3.4 index, to show that positive SST anomalies are positively correlated with $\delta^{18}\text{O}$ at Andean ice core sites. Our results are consistent with these observations, implying that positive tropical SST anomalies can result in a negative phase SAM (weaker polar vortex), which in turn will tend toward enriched $\delta^{18}\text{O}$ and δD values over Antarctica [see *Noone and Simmonds, 2002b*]. The common linkage of the atmospheric circulation in both tropical and polar latitudes to tropical SST anomalies thus provides a plausible explanation for the covariance of Andean and Antarctic stable isotope records.

3.5. Interannual Variability With a High-Pass Filter

[34] Given the interest in using ice cores as proxies to explain the global change record, it is desirable to retain the low-frequency variability of the data, including any long-term trends, as done in the previous two sections. Such an analysis has at least two advantages when considering ice core records and their relationship to climate variability. First, it is well known that ice core records contain a lot of noise (from dating uncertainty and physical factors), especially on the annual timescale, and thus it can be advantageous to use time averages before seeking relationships among ice core records. Second, it is generally assumed that climate anomalies are more coherent geographically as the timescale increases, and therefore sparsely distributed records should become more representative of large-scale climate changes with increasing timescale [e.g., *Moberg et al., 2005; Jones et al., 1997*]. However, we must also recognize that the patterns discussed above may in part be driven by shared trends, whether or not the shared trends are physically linked. Furthermore, much of the variance in isotopic records is imparted on high-frequency timescales, from storm events to seasons to interannual variability, so it is important to understand the isotopic signal at high frequencies.

[35] To address the impact of these factors on our results, we construct a high-pass filtered isotope database, starting with the annual data. These are smoothed with a 5-year running mean, and the smoothed data are subtracted from the original data to yield the high-passed data. This procedure effectively removes the long-term linear trends as well as the interdecadal variability. The data are then renormalized and subject to the same EOF analysis as above.

[36] The first four EOFs of the high-pass isotope data explain similar amounts of variance as the nonfiltered data. PC1, explaining 13% of the variance, is again associated with the central Greenland records (Table 2). PC2, explaining 9% of the variance, corresponds most strongly with West Antarctic records. The effect of removing the low-frequency variability is that the anticorrelation between north Greenland records and West Antarctic records is no longer evident. This is to be expected, since the north Greenland records exhibit a downward trend for the second half of the twentieth century, while the West Antarctic records exhibit an upward trend that was removed by the filter. PC3 of the high-pass filtered data explains 7% of the variance, and suggests a possible connection between Greenland and Antarctic records. The largest correlations, however, are with the James Ross Island and ITASE 02-4 records in Antarctica, which are correlated with PC3 in the opposite sense. PC4 of high-pass filtered data explains 6% of the variance, and, involves a few Antarctic cores, Everest, Mt Logan, and Quelccaya.

[37] To construct the regression patterns discussed in this section and displayed in Figure 6, the climate indices and the SLP and SST data were high-passed filtered in the same manner as the isotope data. The first regression pattern in SLP is again well correlated with the NAO pattern, with a wave-like feature across the northern polar latitudes. In contrast to the nonfiltered pattern, there is not a corresponding wave-like feature in the southern high latitudes associated with PC1. In SST, the anomalies are rather weak, but are certainly NAO-like along 60°N in the North Atlantic.

[38] Filtered isotope PC2 has the weakest anomalies in SLP and SST of any of the regression patterns, suggesting that the low-frequency variability and the trends were important in explaining the relationship. The Southern Hemisphere wave number-3 pattern is still weakly evident in SLP, and there is little structure in the SST.

[39] In contrast, filtered isotope PC3 has strong associations with known SLP and SST patterns, resembling the SOI patterns in both SLP and SST, with weaker but still good correlations with the NPI-related patterns. The SST spatial correlation is remarkably good (Table 3). Correlation is also good with the ENSO-like SAM SST pattern. The SST field at this timescale seems to display only one fundamental pattern, with the location of strongest anomalies reflecting where the atmospheric index is measured. However, there are no SST data from the high-latitude SH, so we may be missing some aspects of the patterns. Comparing the Pacific SOI SST anomalies between the filtered and the nonfiltered data, the largest higher-frequency anomalies are concentrated in a narrow band along the equator, while the anomalies reflecting low-frequency variability are more zonally spread out. This difference was described by *Zhang et al. [1996]* as a key difference between interannual ENSO and interdecadal “ENSO-like” variability in global SST.

[40] Filtered isotope PC4 reflects the SAM in SLP, however the spatial correlation is somewhat weaker than found with nonfiltered data. In SST, the PC4 regression pattern is well correlated with all of the SST patterns, which we have noted are similar to one another.

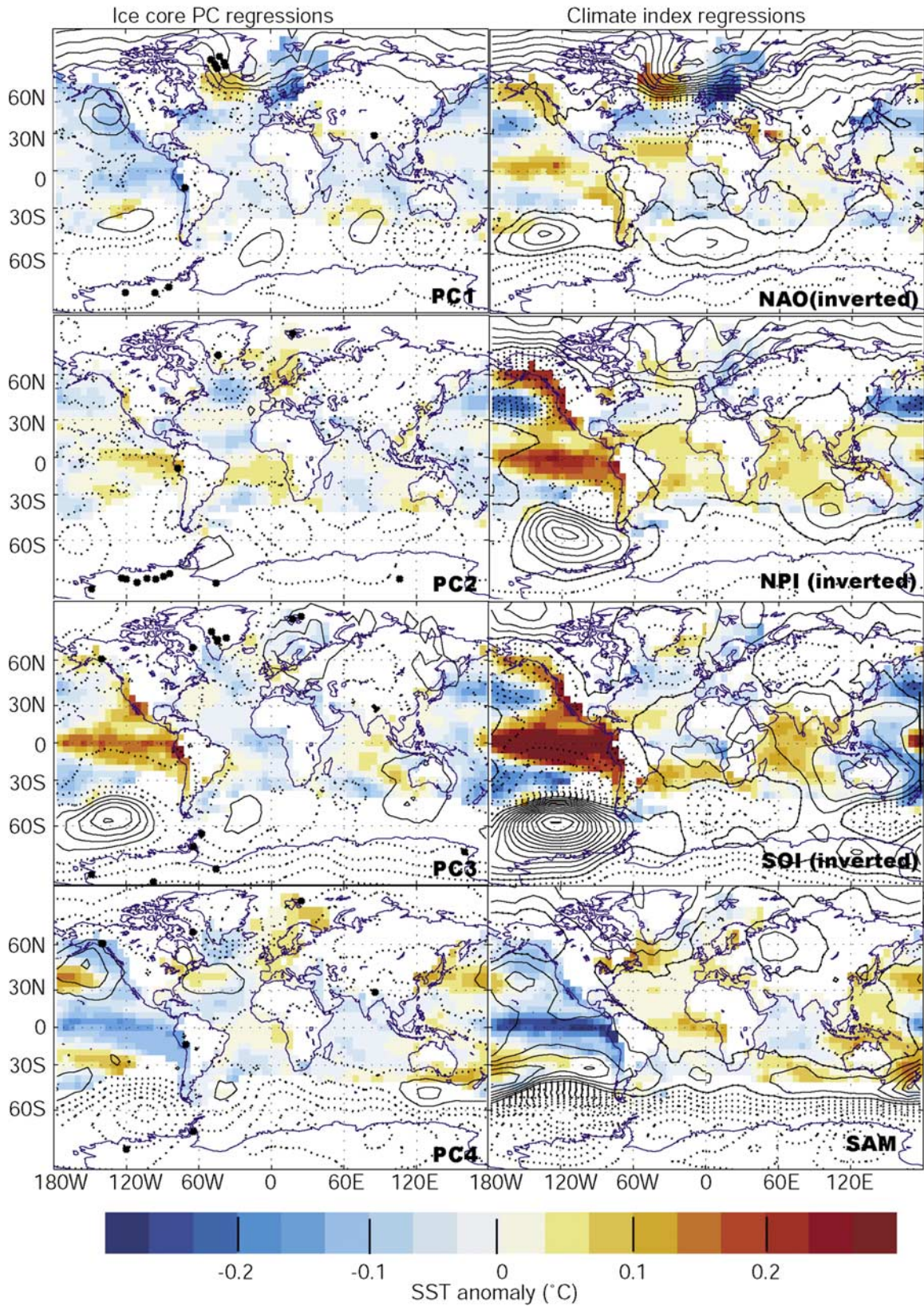


Figure 6. As in Figure 5 but for high-pass filtered data. The ice core annual data, the SLP and SST data, and the climate indices have all been high-passed filtered in the same manner as described in the text.

Table 4. Correlation of the Spatial Pattern of Trends in SLP and SST (Not Shown) With the Pattern Associated With the Indicated Index

	NAO	NPI	SAM	SOI	PC1	PC2	PC3	PC4
SLP	-0.45	-0.36	0.91	0.26	0.50	0.11	0.86	0.76
SST	0.32	-0.23	0.63	0.16	0.13	0.08	0.26	0.31

3.6. Summary of Interannual Variability

[41] The first isotope PC correlates well with cores from central Greenland, and seems to most strongly reflect atmospheric variability associated with the NAO, and only weakly the SST anomalies. The second isotope PC reflects common variability among a set of cores from West Antarctica that are influenced by the wave-3 pattern with a center of action located near 60°S. There is generally a positive trend in these records, which facilitates an association with records that have the opposite trend in North Greenland, a relationship reflected in the analyses of 5-year smoothed and annually averaged data, but not in the analysis of high-passed filtered data. The third isotope PC is well correlated with both the SOI and NPI patterns in SLP and SST, with the SST correlations being somewhat stronger. These correlations are found whether or not the data are filtered, though the high-passed filtered comparisons are somewhat stronger. PC3 involves some of the cores that are usually more difficult to interpret in that they are not obviously dominated by the NAO or the SAM. Thus it is remarkable that the SST signal associated with ENSO comes out so strongly in this analysis. Isotope PC4 contains a SAM signal that is most evident in the SLP regression when the low frequencies are retained. The regression patterns of isotope PC4 do correlate with the trend patterns in SLP and SST (Table 4), however the SAM-like pattern is evident even when the low frequencies are removed. The trend pattern in SLP is SAM-like (not shown), and probably cannot be trusted because of the lack of data over Antarctica. The SAM SST signal is not independent of the El Niño signal, so isotope PC4 is also correlated with an El Niño-like SST pattern. This SST pattern may reflect an important part of the mechanism linking the climate of the high and low latitudes.

3.7. Temporal Variability

[42] In this paper, we have largely focused on spatial patterns, rather than on the reconstruction of climate indices. Such indices include the NAO, NPI, SAM, and SOI. In Table 5 we summarize the correlations of these indices with the isotope PCs. The correlations with the NAO and SAM indices of PC1 and PC4, respectively, are consistent with the spatial patterns discussed above. However, they are somewhat weak, and, not by themselves convincing enough to merit reconstruction of the indices from the raw covariance patterns of the stable isotopes. Normally, a reconstruction would optimize the combination of cores that best describes the observed index, and reconstruction would proceed on the assumption that this optimal combination is stable through time. Our results show that by using a direct EOF approach, spatial patterns can be better resolved than the time series describing the amplitude of the patterns. The climate indices represent a point measurement, or set of

points, rather than the variance of an entire field, and as such are a simplified representation of the pattern. This problem can be somewhat rectified by projecting the patterns onto the observed field to construct a new temporal index [e.g., *Quadrelli and Wallace, 2004*]. These results support suggestions that isotopic variations reflect spatially organized atmospheric and SST patterns as much or more than local meteorological conditions [e.g., *Noone and Simmonds, 2002b; Schmidt et al., 2007*].

4. Discussion and Conclusion

[43] Ice core stable isotopes clearly record climate variability over a wide range of spatial and temporal scales. The ice core records are affected by biases from the timing of precipitation, blowing snow, diffusion, uncertainty in time-scales and other factors, and therefore may be far from the idealized records simulated by models. All of these factors can contribute to the amount of variance unexplained by our analyses. The strongest spatial patterns in stable isotopes (at least in the high latitudes) are associated with the annular modes in the atmospheric circulation. Both high- and low-latitude isotopes contain a component of Pacific climate variability, as characterized by ENSO and the PNA/NPI. Regional patterns are also evident, such as the cooling signal in northwest Greenland and the wave-3 pattern in West Antarctica.

[44] These results are promising for several reasons. First, there is significant covariance among isotopic records. This could be anticipated from the long-established study of atmospheric teleconnections and related modes of variability; however it need not be the case, and has previously been addressed largely on qualitative grounds. Second, ice cores contain a significant component of the global change signal, and therefore can be used to compliment and expand the primarily NH reconstructions based largely on tree rings. Third, although a systematic data-model comparison is beyond the scope of this study, there is a strong apparent agreement among the leading isotope patterns in models and those actually observed. As there is both significant regional and globally relevant information in ice cores, our results highlight the value of obtaining multiple records from many locations, and of repeat drilling to extend existing records. One application of new records and modeling efforts, for example, would be to form a better representation of the global change signal, which may then be projected back in time with solid physical constraints.

[45] Our results are similar using annual resolution records and 5-year averages, suggesting that time averaging is not necessarily the most prudent strategy for reducing

Table 5. Temporal Correlations Between Ice Core Annual PCs and Climate Indices, 1895–1990 (1900–1990 for NPI)^a

	Interannual				High-Pass Filtered			
	NAO	NPI	SAM	SOI	NAO	NPI	SAM	SOI
PC1	-0.34	-0.18	0.04	0.01	-0.26	0.02	0.08	-0.04
PC2	0.13	-0.37	0.01	-0.06	0.21	-0.25	-0.13	0.07
PC3	-0.17	-0.11	-0.09	-0.12	-0.02	0.13	-0.24	-0.32
PC4	0.12	0.17	0.27	0.27	0.25	0.16	0.19	0.21

^aValues in bold type are significant at the 95% level or better by a two-tailed t-test accounting for autocorrelation.

noise. Specifically, there is information in the high frequencies that is signal in the context of this analysis and need not be smoothed out by averaging. It is the strategy for sampling cores in the spatial domain and for averaging or stacking records that drives the amount of variance explained in the data and the amount that can be confidently linked with large-scale climate patterns. A similar conclusion was reached by *Fisher et al.* [1996], based on a thorough analysis of signal versus noise in several Greenland and Canadian Arctic ice cores.

[46] A recent comparison of modeled isotopes with observations from the Global Network for Isotopes in Precipitation (GNIP) database [*Hoffmann et al.*, 2005] suggested that models may be overoptimistic with respect to the interannual climate information that can be extracted from ice core isotope records. However, we have shown that the annual NAO and SAM signals are robust in the ice core database. *Hoffmann et al.* [2005] also support the stacking of ice cores to increase signal-to-noise ratios. Our database includes a few stacks encompassing a relatively small field area such as those of *White et al.* [1997], *Fisher and Koerner* [1994], and *Fisher et al.* [1995] in Greenland, Dronning Maud in Antarctica [*Graf et al.*, 2002], and the Quelccaya 2003 and 1983 cores [*Thompson et al.*, 2006a]. Indeed, these stacked records have signals that are highly weighted in our EOF analyses. However, comparable unstacked records, such as the PARCA D2 and D3 cores, are also heavily weighted by the EOFs, suggesting that individual records are useful. Without the use of individual records, it would be hard to notice the differences in the Greenland signal at say, NGRIP, GITS, and Summit. Thus a regional stack may mask some important differences, which we highlighted by comparing a simple Arctic mean with the leading principal components. From a practical standpoint, it is often expensive and logistically impossible to obtain several temporally overlapping ice cores across a broad area. Before stacking, it is important to consider the complexity of the isotopic signal across the area, in relation to the climate signal one is ultimately seeking to represent. For the NAO, in a model, *Schmidt et al.* [2007] find a difference in the sensitivity of isotopes at Summit and NGRIP, with a higher sensitivity at NGRIP, in agreement with our results.

[47] Models have not demonstrated that an idealized globally averaged isotope record would mimic the global temperature record. Such a result is not necessarily expected, since there will be some regions where depletion is the response to changes in the mean climate. For instance, in the tropics, it is thought that convection dominates the isotopic signal [e.g., *Worden et al.*, 2007], and therefore increasing convection with a warming climate will lead to depletion. At some high-latitude sites, such as Mt Logan, changes from zonal transport and local moisture sources to meridional transport and distant moisture sources, are hypothesized to have contributed to large shifts toward depleted values in the nineteenth century [*Fisher et al.*, 2004]. Possibly, a similar mechanism explains the James Ross Island twentieth-century depletion, which is not correlated with Antarctic Peninsula region temperatures [*Aristarain et al.*, 1990; *Mosley-Thompson and Thompson*, 2003; *Vaughan et al.*, 2003]. The high correlation of our analysis of 5-year averaged isotope records with the global

temperature record is therefore an intriguing result. Moreover, our analyses find that the correlation is stronger with the global record than with the NH or SH mean or the NH land-only temperature, or the globally averaged SST record (not shown). This seems to stem in part from the shared biases in the global temperature and our ice core database. That is to say the global temperature record is dominated by variability in Northern Hemisphere land temperatures, which in turn are strongly influenced by the NAO/NAM [e.g., *Hurrell*, 1996]. Likewise, SH temperatures have a component of SAM variability. Therefore ice core records with strong NAO and SAM signals go a long way toward explaining the global temperature record. A question worthy of further study is why low-latitude Tibetan cores, especially Dundee and Dasuopu, show pronounced twentieth-century enrichment, and therefore contribute to the global change signal in our database. These ice core records are consistent with the local temperature records [*Yao et al.*, 2006], but are not well understood from modeling efforts. The more northern sites, like Dundee, are thought to be more temperature-dominated, while the more southern sites, like Dasuopu, are thought to be more dominated by the monsoon [e.g., *Tian et al.*, 2003].

[48] Our results pose new targets for isotope modeling investigations. Using only water isotopes has the advantage of covariance patterns being directly comparable with results from isotope-enabled general circulation models. This potentially eliminates a common step in data-model comparison, which is to compare model-simulated temperature and other variables to proxy-estimated temperature or other climate parameters. To this end, because this work uses a network of proxies, it moves away from simple local regression interpretations and calibrations of ice cores and instead targets an integrative assessment that accounts for systematic variations in the circulation and climatic conditions. Since isotopes are well modeled, the physical mechanisms that lead to the empirically derived patterns can be understood using the diagnostic capabilities afforded by systematic sets of model simulations. In this way, much can be learned about the behavior of the physical system that should be applicable to timescales beyond the last century. These results may then provide practical guidance for coordinated ice core drilling efforts. With new data and modeling efforts, paleoclimate reconstructions can be accompanied by a rigorous and physical explanation of what the proxies record.

[49] **Acknowledgments.** We would like to thank all of the ice core data contributors and their research and field teams, who have devoted a lot of time and energy to producing these valuable data. We also thank the World Data Center for Paleoclimatology and the National Snow and Ice Data center for archiving large amounts of ice core data, as well as NOAA, NCAR and the Hadley Centre for making the meteorological data available. Several U.S. and international agencies have funded these projects, including NASA, NOAA and NSF. Some funding for the first author was from NSF grant OPP-0440414. We would like to thank Eric Steig for his helpful comments on a draft of this manuscript and two reviewers for making constructive suggestions that led to improvement of the manuscript.

References

- Allan, R., and T. Ansell (2006), A new globally complete monthly historical gridded mean sea level pressure data set (HadSLP2): 1850–2004, *J. Clim.*, 19(22), 5816–5842.
- Andersen, K. K., P. D. Ditlevsen, S. O. Rasmussen, H. B. Clausen, B. M. Vinther, and S. J. Johnsen (2006), Retrieving a common accumulation

- record from Greenland ice cores for the past 1800 years, *J. Geophys. Res.*, *111*, D15106, doi:10.1029/2005JD006765.
- Anklin, M., R. C. Bales, E. Mosely-Thompson, and K. Steffen (1998), Annual accumulation at two sites in northwest Greenland during recent centuries, *J. Geophys. Res.*, *103*(D22), 28,775–28,783.
- Aristarain, A. J., J. Jouzel, and C. Lorius (1990), A 400 years isotope record of the Antarctic Peninsula climate, *Geophys. Res. Lett.*, *17*(13), 2369–2372.
- Baldwin, M. P. (2001), Annular modes in global daily surface pressure, *Geophys. Res. Lett.*, *28*(21), 4115–4118.
- Box, J. E. (2002), Survey of Greenland instrumental temperature records: 1873–2001, *Int. J. Climatol.*, *22*, 1829–1847.
- Bradley, R. S., M. Vuille, D. Hardy, and L. G. Thompson (2003), Low latitude ice cores record Pacific sea surface temperatures, *Geophys. Res. Lett.*, *30*(4), 1174, doi:10.1029/2002GL016546.
- Bretherton, C. S., C. Smith, and J. M. Wallace (1992), An intercomparison of methods for finding coupled patterns in climate data, *J. Clim.*, *5*, 541–560.
- Brohan, P., J. J. Kennedy, I. Harris, S. F. B. Tett, and P. D. Jones (2006), Uncertainty estimates in regional and global observed temperature changes: A new dataset from 1850, *J. Geophys. Res.*, *111*, D12106, doi:10.1029/2005JD006548.
- Burger, G., I. Fast, and U. Cubasch (2006), Climate reconstruction by regression—32 variations on a theme, *Tellus, Ser. A*, *58*, 227–235.
- Chapman, W. L., and J. E. Walsh (1993), Recent variations of sea-ice and air temperature in high-latitudes, *Bull. Am. Meteorol. Soc.*, *74*(1), 33–47.
- Chylek, P., J. E. Box, and G. Lesins (2004), Global warming and the Greenland ice sheet, *Clim. Change*, *63*(1–2), 201–221.
- Cole, J. E., D. Rind, R. S. Webb, J. Jouzel, and R. Healy (1999), Climatic controls on interannual variability of precipitation $\delta^{18}\text{O}$: Simulated influence of temperature, precipitation amount, and vapor source region, *J. Geophys. Res.*, *104*(D12), 14,223–14,235.
- D'Arrigo, R., R. Wilson, and G. Jacoby (2006), On the long-term context for late twentieth century warming, *J. Geophys. Res.*, *111*, D03103, doi:10.1029/2005JD006352.
- Ekaykin, A., V. Y. Lipenkov, N. I. Barkov, J. R. Petit, and V. Masson-Delmotte (2002), Spatial and temporal variability in isotopic composition of recent snow in the vicinity of Vostok Station, Antarctica: Implications for ice-core record interpretation, *Ann. Glaciol.*, *35*, 181–186.
- Esper, J., E. R. Cook, and F. H. Schweingruber (2002), Low-frequency signals in long tree-ring chronologies for reconstructing past temperature variability, *Science*, *295*, 2250–2253.
- Esper, J., D. C. Frank, R. J. S. Wilson, and K. R. Briffa (2005), Effect of scaling and regression on reconstructed temperature amplitude for the past millennium, *Geophys. Res. Lett.*, *32*, L07711, doi:10.1029/2004GL021236.
- Fisher, D. A. (2002), High-resolution multiproxy climatic records from ice cores, tree-rings, corals and documentary sources using eigenvector techniques and maps: Assessment of recovered signal and errors, *Holocene*, *12*(4), 401–419.
- Fisher, D. A., and R. M. Koerner (1994), Signal and noise in four ice core records from the Agassiz ice cap, Ellesmere Island, NWT, Canada, *Holocene*, *4*(1), 113–120.
- Fisher, D. A., R. M. Koerner, and N. Reeh (1995), Holocene climatic records from Agassiz ice cap, Ellesmere Island, NWT, Canada, *Holocene*, *5*(1), 19–24.
- Fisher, D. A., R. M. Koerner, K. Kuivinen, H. B. Clausen, S. J. Johnsen, J. P. Steffensen, N. Gundestrup, and C. U. Hammer (1996), Intercomparison of ice core $\delta^{18}\text{O}$ and precipitation records from sites in Canada and Greenland over the last 3500 years and over the last few centuries in detail using EOF techniques, in *Climatic Variations and Forcing Mechanisms of the Last 2000 Years*, edited by P. D. Jones et al., pp. 297–328, Springer, New York.
- Fisher, D. A., et al. (2004), Stable isotope records from Mount Logan, Eclipse ice cores and nearby Jellybean Lake. Water cycle of the North Pacific over 200 years and over five vertical kilometers: Sudden shifts and tropical connections, *Geograph. Phys. Quat.*, *58*(2–3), 337–352.
- Fyfe, J. C., G. J. Boer, and G. M. Flato (1999), The Arctic and Antarctic Oscillations and their projected changes under global warming, *Geophys. Res. Lett.*, *26*(11), 1601–1604.
- Goto-Azuma, K., R. M. Koerner, and D. A. Fisher (2002), An ice core record over the last two centuries from Penny Ice Cap, Baffin Island, Canada, *Ann. Glaciol.*, *35*, 29–35.
- Graf, W., H. Oerter, O. Reinwarth, W. Stichler, F. Wilhelms, H. Miller, and R. Mulvaney (2002), Stable isotope records from Dronning Maud Land, Antarctica, *Ann. Glaciol.*, *35*, 195–201.
- Hartmann, D. L., J. M. Wallace, V. Limpasuvan, D. W. J. Thompson, and J. R. Holton (2000), Can ozone depletion and global warming interact to produce rapid climate change?, *Proc. Natl. Acad. Sci. U. S. A.*, *97*(4), 1412–1417.
- Hoffmann, G., M. Cuntz, M. Werner, and J. Jouzel (2005), A systematic comparison between the IAEA/GNIP isotope network and Atmospheric General Circulation Models: How much climate information is in the water isotopes?, in *Isotopes in the Water Cycle—Past, Present and Future of a Developing Science*, edited by P. K. Aggarwal, J. R. Gat, and K. F. O. Froehlich, pp. 303–320, Springer, New York.
- Holdsworth, G., H. R. Krouse, and M. Nosal (1992), Ice core climate signals from Mount Logan, Yukon, A. D. 1700–1987, in *Climate Since AD 1500*, edited by R. S. Bradley and P. D. Jones, pp. 483–504, Routledge, Boca Raton, Fla.
- Hurrell, J. W. (1995), Decadal trends in the North-Atlantic Oscillation—Regional temperatures and precipitation, *Science*, *269*(5224), 676–679.
- Hurrell, J. W. (1996), Influence of variations in extratropical teleconnections on Northern Hemisphere temperature, *Geophys. Res. Lett.*, *23*(6), 665–668.
- Isaksson, E., D. Divine, J. Kohler, T. Martma, V. Pohjola, H. Motoyama, and O. Watanabe (2005), Climate oscillations as recorded in Svalbard ice core $\delta^{18}\text{O}$ records between AD 1200 and 1997, *Geogr. Ann., Ser. A*, *87*(1), 203–214.
- Jacobel, R. W., B. C. Welch, E. J. Steig, and D. P. Schneider (2005), Glaciological and climatic significance of Hercules Dome, Antarctica: An optimal site for deep ice core drilling, *J. Geophys. Res.*, *110*, F01015, doi:10.1029/2004JF000188.
- Jones, J. M., and M. Widmann (2004), Early peak in Antarctic Oscillation Index, *Nature*, *432*, 290–291.
- Jones, P. D., and M. E. Mann (2004), Climate over past millennia, *Rev. Geophys.*, *42*, RG2002, doi:10.1029/2003RG000143.
- Jones, P. D., T. J. Osborn, and K. R. Briffa (1997), Estimating sampling errors in large-scale temperature averages, *J. Clim.*, *10*, 2548–2568.
- Kaplan, A., M. Cane, Y. Kushnir, A. Clement, M. Blumenthal, and B. Rajagopalan (1998), Analyses of global sea surface temperature 1856–1991, *J. Geophys. Res.*, *103*, 18,567–18,589.
- L'Heureux, M. L., and D. W. J. Thompson (2006), Observed relationships between the El-Niño/Southern Oscillation and the extratropical zonal-mean circulation, *J. Clim.*, *19*, 276–287.
- Mann, M. E., R. S. Bradley, and M. K. Hughes (1998), Global-scale temperature patterns and climate forcing over the past six centuries, *Nature*, *392*, 779–787.
- Mayewski, P. A., et al. (2004), A 700-year record of Southern Hemisphere extratropical climate variability, *Ann. Glaciol.*, *39*, 127–132.
- Mayewski, P. A., et al. (2005), The International Trans-Antarctic Scientific Expedition (ITASE): An overview, *Ann. Glaciol.*, *41*, 180–185.
- Mo, K. C. (2000), Relationships between low-frequency variability in the Southern Hemisphere and sea surface temperature anomalies, *J. Clim.*, *13*, 3599–3610.
- Moberg, A., D. M. Sonechkin, K. Holmgren, N. M. Datsenko, and W. Karlen (2005), Highly variable Northern Hemisphere temperatures reconstructed from low- and high-resolution proxy data, *Nature*, *433*, 613–617.
- Moore, G. W. K., G. Holdsworth, and K. Alverson (2002), Climate change in the North Pacific region over the past three centuries, *Nature*, *420*, 401–403.
- Mosley-Thompson, E., and L. G. Thompson (2003), Ice core paleoclimate histories from the Antarctic Peninsula: Where do we go from here?, in *Antarctic Peninsula Climate Variability: Historical and Paleoenvironmental Perspectives*, edited by E. Domak, et al., 260 pp., *Antarctic Res. Ser.*, vol. 79, AGU, Washington, D. C.
- Mosley-Thompson, E., L. G. Thompson, P. M. Grootes, and N. Gundestrup (1990), Little Ice Age (Neoglacial) paleoenvironmental conditions at Siple Station, Antarctica, *Ann. Glaciol.*, *14*, 199–204.
- Mosley-Thompson, E., L. G. Thompson, and P.-N. Lin (2006), A multi-century ice-core perspective on 20th-century climate change with new contributions from high-Arctic and Greenland (PARCA) cores, *Ann. Glaciol.*, *43*, 42–47.
- Mulvaney, R., H. Oerter, D. A. Peel, W. Graf, C. Arrowsmith, E. C. Pasteur, B. Knight, G. C. Littot, and W. D. Miners (2002), 1000 year ice-core records from Berkner Island, Antarctica, *Ann. Glaciol.*, *35*, 45–51.
- Noone, D. C., and I. Simmonds (2002a), Associations between $\delta^{18}\text{O}$ of water and climate parameters in a simulation of atmospheric circulation for 1979–95, *J. Clim.*, *15*, 3150–3169.
- Noone, D. C., and I. Simmonds (2002b), Annular variations in moisture transport mechanisms and the abundance of $\delta^{18}\text{O}$ in Antarctic Snow, *J. Geophys. Res.*, *107*(D24), 4742, doi:10.1029/2002JD002262.
- North, G. R., T. L. Bell, and R. F. Cahalan (1982), Sampling errors in the estimation of empirical orthogonal functions, *Mon. Weather Rev.*, *110*, 699–706.
- Patterson, W. S. B., R. M. Koerner, D. A. Fisher, S. J. Johnsen, H. B. Clausen, W. Dansgaard, P. Bucher, and H. Oeschger (1977), An oxygen-isotope climatic record from Devon Island ice cap, Arctic Canada, *Nature*, *266*(5602), 508–511.

- Petit, J. R., et al. (1999), Climate and atmospheric history of the past 420,000 years from the Vostok ice core, Antarctica, *Nature*, 399, 429–436.
- Quadrelli, R., and J. M. Wallace (2004), A simplified linear framework for interpreting patterns of Northern Hemisphere wintertime climate variability, *J. Clim.*, 17, 3728–3744.
- Ribera, P., and M. E. Mann (2003), ENSO related variability in the Southern Hemisphere, 1948–2000, *Geophys. Res. Lett.*, 30(1), 1006, doi:10.1029/2002GL015818.
- Schmidt, G. A., A. N. LeGrande, and G. Hoffmann (2007), Water isotope expressions of intrinsic and forced variability in a coupled ocean-atmosphere model, *J. Geophys. Res.*, 112, D10103, doi:10.1029/2006JD007781.
- Schneider, D. P., E. J. Steig, and J. C. Comiso (2004), Recent climate variability in Antarctica from satellite-derived temperature data, *J. Clim.*, 17, 1569–1583.
- Schneider, D. P., E. J. Steig, and T. van Ommen (2005), High-resolution ice core stable isotopic records from Antarctica: Towards interannual climate reconstruction, *Ann. Glaciol.*, 41, 63–70.
- Schneider, D. P., E. J. Steig, T. D. van Ommen, D. A. Dixon, P. A. Mayewski, J. M. Jones, and C. M. Bitz (2006), Antarctic temperatures over the past two centuries from ice cores, *Geophys. Res. Lett.*, 33, L16707, doi:10.1029/2006GL027057.
- Shindell, D. T., and G. A. Schmidt (2004), Southern Hemisphere climate response to ozone changes and greenhouse gas increases, *Geophys. Res. Lett.*, 31, L18209, doi:10.1029/2004GL020724.
- Shugui, H., Q. Dahe, Y. Tandong, Z. Dongqi, and C. Tuo (2002), Recent change of the ice core accumulation rates in the Qing-Tibetan Plateau, *Chin. Sci. Bull.*, 47(20), 1746–1749.
- Sjoukje, P., and G. J. van Oldenborgh (2006), Shifts in ENSO coupling processes under global warming, *Geophys. Res. Lett.*, 33, L11704, doi:10.1029/2006GL026196.
- Steig, E. J., et al. (2005), High-resolution ice cores from US-ITASE (West Antarctica): Development and validation of chronologies and determination of precision and accuracy, *Ann. Glaciol.*, 41, 77–84.
- Stenni, B., M. Proposito, R. Gragnani, O. Flora, J. Jouzel, S. Falourd, and M. Frezzotti (2002), Eight centuries of volcanic signal and climate change at Talos Dome (East Antarctica), *J. Geophys. Res.*, 107(D9), 4076, doi:10.1029/2000JD000317.
- Thompson, D. W. J., and S. Solomon (2002), Interpretation of recent Southern Hemisphere climate change, *Science*, 296, 895–899.
- Thompson, L. G., E. Mosley-Thompson, J. F. Bolzan, and B. R. Koci (1985), A 1500 year record of tropical precipitation recorded in ice cores from the Quelccaya Ice Cap, Peru, *Science*, 229(4717), 971–973.
- Thompson, L. G., E. Mosley-Thompson, M. E. Davis, J. F. Bolzan, J. Dai, T. Yao, N. Gundestrup, X. Wu, L. Klein, and Z. Xie (1989), Holocene-Late Pleistocene climatic ice core records from Qinghai-Tibetan Plateau, *Science*, 246, 474–477.
- Thompson, L. G., E. Mosley-Thompson, R. Mulvaney, J. Dai, P. N. Lin, M. E. Davis, and C. F. Raymond (1994), Climate since AD 1510 on Dyer Plateau, Antarctic Peninsula: Evidence for recent climate change, *Ann. Glaciol.*, 20, 420–426.
- Thompson, L. G., E. Mosley-Thompson, M. E. Davis, P.-N. Lin, K. A. Henderson, J. Cole-Dai, J. F. Bolzan, and K.-B. Liu (1995), Late glacial stage and Holocene tropical ice core records from Huascarán, Peru, *Science*, 269, 46–50.
- Thompson, L. G., T. Yao, M. E. Davis, K. A. Henderson, E. Mosley-Thompson, P.-N. Lin, J. Beer, H.-A. Synal, J. Cole-Dai, and J. F. Bolzan (1997), Tropical climate instability: The last glacial cycle from a Qinghai-Tibetan ice core, *Science*, 276, 1821–1825.
- Thompson, L. G., et al. (1998), A 25,000 year tropical climate history from Bolivian ice cores, *Science*, 282(5295), 1858–1864.
- Thompson, L. G., T. Yao, E. Mosley-Thompson, M. E. Davis, K. A. Henderson, and P.-N. Lin (2000), A high-resolution millennial record of the South Asian Monsoon from Himalayan ice cores, *Science*, 298, 1916–1919.
- Thompson, L. G., E. Mosley-Thompson, H. Brecher, M. Davis, B. Leon, D. Les, P.-N. Lin, T. Mashiotta, and K. Mountain (2006a), Abrupt tropical climate change: Past and present, *Proc. Natl. Acad. Sci. U. S. A.*, 103, 10,536–10,543.
- Thompson, L. G., Y. Tandong, M. E. Davis, E. Mosley-Thompson, T. A. Mashiotta, P.-N. Lin, V. N. Mikhelenko, and V. S. Zagorodnov (2006b), Holocene climate variability archived in the Puruogangri ice cap on the central Tibetan Plateau, *Ann. Glaciol.*, 43, 61–69.
- Tian, L., T. Yao, P. F. Schuster, J. W. C. White, K. Ichiyanagi, E. Pendall, J. Pu, and W. Yu (2003), Oxygen-18 concentrations in recent precipitation and ice cores on the Tibetan Plateau, *J. Geophys. Res.*, 108(D9), 4293, doi:10.1029/2002JD002173.
- Trenberth, K. E. (1984), Signal versus noise in the Southern Oscillation, *Mon. Weather Rev.*, 112, 326–332.
- Trenberth, K. E., and J. W. Hurrell (1994), Decadal atmosphere-ocean variations in the Pacific, *Clim. Dyn.*, 9(6), 303–319.
- Trenberth, K. E., and B. L. Otto-Bliesner (2003), Toward integrated reconstruction of past climate, *Science*, 300, 589–591.
- Trenberth, K. E., D. P. Stepaniak, and L. Smith (2005), Interannual variability of patterns of atmospheric mass distribution, *J. Clim.*, 18, 2812–2824.
- Turner, J. T., J. E. Overland, and J. E. Walsh (2007), An Arctic and Antarctic perspective on recent climate change, *Int. J. Climatol.*, 27, 277–293.
- van Ommen, T. D., and V. Morgan (1997), Calibrating the ice core paleothermometer using seasonality, *J. Geophys. Res.*, 102(D8), 9351–9357.
- van Ommen, T. D., V. Morgan, and M. A. J. Curran (2004), Deglacial and Holocene changes in accumulation at Law Dome, *Ann. Glaciol.*, 39, 359–365.
- Vaughan, D. G., et al. (2003), Recent rapid regional climate warming on the Antarctic Peninsula, *Clim. Change*, 60, 243–274.
- Venegas, S. A. (2003), The Antarctic Circumpolar Wave: A combination of two signals?, *J. Clim.*, 16, 2509–2525.
- Vinther, B. M., S. J. Johnsen, K. K. Andersen, H. B. Clausen, and A. W. Hansen (2003), NAO signal recorded in the stable isotopes of Greenland ice cores, *Geophys. Res. Lett.*, 30(7), 1387, doi:10.1029/2002GL016193.
- von Storch, H., and F. W. Zwiers (2001), *Statistical Analysis in Climate Research*, 484 pp., Cambridge Univ. Press, New York.
- von Storch, H., E. Zorita, J. M. Jones, Y. Dimitriev, F. Gonzalez-Rouco, and S. B. Tett (2004), Reconstructing past climate from noisy data, *Science*, 306, 679–682.
- Vuille, M., and M. Werner (2005), Stable isotopes in precipitation recording South American summer monsoon and ENSO variability—observations and model results, *Clim. Dyn.*, 25, 401–413, doi:10.1007/s00382-005-0049-9.
- Vuille, M., R. S. Bradley, M. Werner, and F. Keimig (2003), 20th-century climate change in the tropical Andes, *Clim. Change*, 59, 75–99.
- Vuille, M., M. Werner, R. S. Bradley, and E. Keimig (2005), Stable isotopes in precipitation in the Asian Monsoon region, *J. Geophys. Res.*, 110, D23108, doi:10.1029/2005JD006022.
- Wahl, E. R., D. M. Ritson, and C. M. Ammann (2006), Comment on “Reconstructing past climate from noisy data,” *Science*, 312(5773), 529, doi:10.1126/science1120866.
- Wake, C. P., K. Yalcin, and N. S. Gundestrup (2002), The climate signal recorded in the oxygen-isotope, accumulation and major-ion time series from the Eclipse ice core, Yukon Territory, Canada, *Ann. Glaciol.*, 35, 416–422.
- Wallace, J. M., and D. S. Gutzler (1981), Teleconnections in the geopotential height field during the Northern Hemisphere winter, *Mon. Weather Rev.*, 109, 784–812.
- Wallace, J. M., Y. Zhang, and L. Bajuk (1996), Interpretation of interdecadal trends in Northern Hemisphere surface air temperature, *J. Clim.*, 9, 249–258.
- Werner, M., and M. Heimann (2002), Modelling the interannual variability of water isotopes in Greenland and Antarctica, *J. Geophys. Res.*, 107(D1), 4001, doi:10.1029/2001JD900253.
- White, J. W. C., L. K. Barlow, D. Fisher, P. Grootes, J. Jouzel, S. J. Johnsen, M. Stuiver, and H. Clausen (1997), The climate signal in the stable isotopes of snow from Summit, Greenland: Results of comparisons with modern climate observations, *J. Geophys. Res.*, 102(C12), 26,425–26,439.
- Worden, J. R., D. Noone, K. Bowman, and TES Team Members (2007), Importance of rain evaporation and continental convection in the tropical water cycle, *Nature*, 445, 528–532, doi:10.1038/nature05508.
- Yao, T., Z. Li, L. G. Thompson, E. Mosley-Thompson, Y. Wang, L. Tian, N. Wang, and K. Duan (2006), $\delta^{18}\text{O}$ records from Tibetan ice cores reveal differences in climatic changes, *Ann. Glaciol.*, 43, 1–7.
- Zhang, Y., J. M. Wallace, and N. Iwasaka (1996), Is climate variability over the North Pacific a linear response to ENSO?, *J. Clim.*, 9(7), 1468–1478.
- Zheng, J., D. A. Fisher, E. Blake, G. Hall, J. Vaive, M. Krachler, C. Zdanowicz, J. Lam, G. Lawsons, and W. Shotyk (2006), An ultra-clean firn core from the Devon Island ice cap, Nunavut, Canada, retrieved using a titanium drill specially designed for trace element studies, *J. Environ. Monit.*, 8(3), 406–413.

D. C. Noone, Cooperative Institute for Research in Environmental Sciences, University of Colorado, Boulder, CO 80309-0216, USA.

D. P. Schneider, National Center for Atmospheric Research, Boulder, CO 80307, USA. (dschneid@ucar.edu)